Article

Why Are Water–Hydrophobic Interfaces Charged?

Konstantin N. Kudin, and Roberto Car

J. Am. Chem. Soc., **2008**, 130 (12), 3915-3919 • DOI: 10.1021/ja077205t

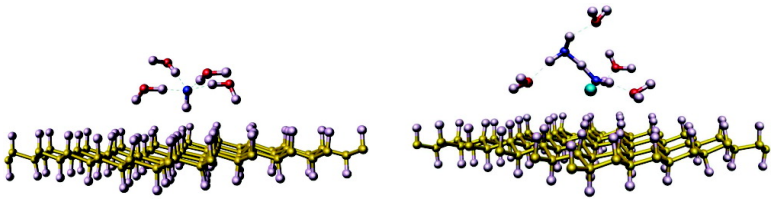

J|A|C|S
ARTICLES
Published on Web 03/01/2008

Why Are Water−Hydrophobic Interfaces Charged?

Konstantin N. Kudin and Roberto Car*

Department of Chemistry and Princeton Institute for Science and Technology of Materials (PRISM), Princeton University, Princeton, New Jersey 08544

Received September 17, 2007; E-mail: rcar@princeton.edu

Abstract: We report ab initio molecular dynamics simulations of hydroxide and hydronium ions near a hydrophobic interface, indicating that both ions behave like amphiphilic surfactants that stick to a hydrophobic hydrocarbon surface with their hydrophobic side. We show that this behavior originates from the asymmetry of the molecular charge distribution which makes one end of the ions strongly hydrophobic while the other end is even more hydrophilic than the regular water (H_2O) molecules. The effect is more pronounced for the hydroxide than for the hydronium. Our results are consistent with several experimental observations and explain why hydrophobic surfaces in contact with water acquire a net negative charge, a phenomenon that has important implications for biology and polymer science.

Introduction

Simple electrostatic considerations suggest that solvated ions would rather be located in the high dielectric constant environment of bulk water than at an interface with a low dielectric medium. Yet experiments reveal that water interfaces with oil droplets, solid hydrophobic polymers, hydrophobic assembled structures, and even gas bubbles are usually negatively charged[1−6] and become positively charged in highly acidic solutions.[7] Detailed analysis of the pH dependence led to attribute the surface charges to hydroxide (OH^-) and hydronium (H^+) ions.[7] Moreover, since hydroniums dominate only at low pH, it was concluded that they have a lower hydrophobic surface affinity than hydroxides.[7] The presence of water ions at hydrophobic interfaces is further supported by spectroscopic studies in highly concentrated solutions, which show that the O−H stretching modes in the vicinity of the liquid−vapor interface are affected by both OH^- and H^+ ions, albeit more substantially by the latter.[8]

To date the microscopic origin of this phenomenon is not understood. Molecular dynamics (MD) simulations based on classical intermolecular potentials predict different results depending on the specific interface under study and classical force field employed. Initially, the suggestion that hydronium might have some preference for the interface has emerged from Monte Carlo simulations of protonated water clusters with a model interatomic potential.[9] Subsequent simulations for the water−air interface found either no surface affinity for H^+[10] or positive affinity for H^+ and negative affinity for OH^-.[11−13] Simulations for OH^- ions only in the presence of a structureless hydrophobic wall found positive hydroxide affinity.[14] Reference 12 also reports short ab initio molecular dynamics (AIMD) simulations for the water−air interface, using a potential derived from quantum mechanical density functional theory. Specifically, the authors observed that at the beginning of a 2 ps AIMD simulation a hydroxide quickly jumped into the interior of a water−air slab and stayed there for the remainder of the simulation.[12] Together with the other data, these results led to conclusions that the water−vapor interface is acidic.[12] The same authors note, however,[13] that this result is seemingly in contradiction with the experimental data that indicate negative surface charge. To study the issue further, in ref 13 clusters containing 47 waters and 1 hydroxide were first sampled by classical MD runs and then optimized at the ab initio DFT level. From these simulations, it was determined that the clusters with hydroxide in the interior tend to have lower energy than those with the hydroxide located at the convex cluster surface. In contrast, static density functional calculations on small clusters found that OH^--water complexes near hydrophobic methyl groups are energetically preferred to bulk hydrated complexes.[15] A general criticism of some of the existing simulation work is that it tends to attribute the surface affinity to the structure of the interfacial water rather than to the specificity of the ions. This does not explain why in the case of a water−hydrophobic

(1) Marinova, K. G.; Alargova, R. G.; Denkov, N. D.; Velev, O. D.; Petsev, D. N.; Ivanov, I. B.; Borwankar, R. P. *Langmuir* **1996**, *12*, 2045.
(2) Stubenrauch, C.; Schlarmann, J.; Strey, R. *Phys. Chem. Chem. Phys.* **2002**, *4*, 4504.
(3) Weidenhammer, P.; Jacobasch, H. J. *J. Colloid Interface Sci.* **1996**, *180*, 232.
(4) Feldman, K.; Hahner, G.; Spencer, N. D.; Harder, P.; Grunze, M. *J. Am. Chem. Soc.* **1999**, *121*, 10134.
(5) Beattie, J. K.; Djerdjev, A. M. *Angew. Chem., Int. Ed. Engl.* **2004**, *43*, 3568.
(6) Beattie, J. K. *Lab Chip* **2006**, *6*, 1409.
(7) Zimmermann, R.; Dukhin, S.; Werner, C. *J. Phys. Chem. B* **2001**, *105*, 8544.
(8) Tarbuck, T. L.; Ota, S. T.; Richmond, G. L. *J. Am. Chem. Soc.* **2006**, *128*, 14519.
(9) Kusaka, I.; Oxtoby, D. W. *J. Chem. Phys.* **2000**, *113*, 10100.
(10) Dang, L. X. *J. Chem. Phys.* **2003**, *119*, 6351.
(11) Mucha, M.; Frigato, T.; Levering, L. M.; Allen, H. C.; Tobias, D. J.; Dang, L. X.; Jungwirth, P. *J. Chem. Phys. B* **2005**, *109*, 7617.
(12) Buch, V.; Milet, A.; Vacha, R.; Jungwirth, P.; Devlin, J. P. *Proc. Natl. Acad. Sci.* **2007**, *104*, 7342.
(13) Vacha, R.; Buch, V.; Milet, A.; Devlin, J. P; Jungwirth P. *Phys. Chem. Chem. Phys.* **2007**, *9*, 4736.
(14) Zangi, R.; Engberts, J. B. F. N. *J. Am. Chem. Soc.* **2005**, *127*, 2272.
(15) Kreuzer, H. J.; Wang, R. L. C.; Grunze, M. *J. Am. Chem. Soc.* **2003**, *125*, 8384.

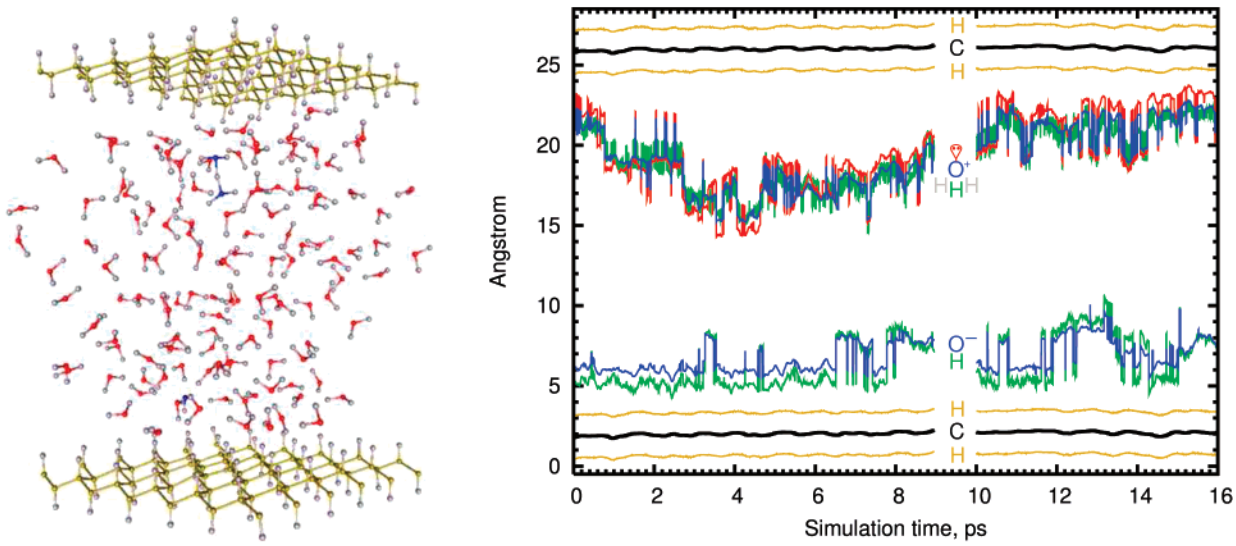

Figure 1. (a) System layout from a snapshot of the simulation. The three-dimensional periodic simulation cell contains 127 water molecules, 1 hydronium H^+, 1 hydroxide OH^-, and 1 fully hydrogenated graphene sheet (6 × 6 supercell, 72 C and 72 H atoms). For clarity we also show a periodic replica of the hydrophobic sheet. The two oxygens participating in the Zundel form of the hydronium and the hydroxide oxygen are shown in blue. The cell is hexagonal in the graphene plane (side 15.265 Å), with the vertical dimension of 24 Å. (b) Time evolution (blue line) of the vertical position of the hydroxide oxygen and of the hydronium oxygen. Two trajectories are shown, the second one starting at $t = 10$ ps. The hydroxide is in the lower part of the figure; the hydronium is in the upper part. The lateral displacement occurring in each proton jump does not appear in the figure. The coloring scheme is provided in the space between the two trajectories. Specifically, the positions of the hydroxide hydrogen and of the most distant hydrogen covalently bonded to O_{H^+} are shown in green. When the hydronium has the Zundel form, this hydrogen is shared between two oxygens. The position of the O_{H^+} lone pair is shown in red. The direction of the lone pair is set by the vector originating from O_{H^+}, which forms equal angles with the three directions defined by the hydrogens. This definition is identical with the π-orbital axis vector (POAV) analysis in pyramidal molecules.[45] For visual guidance, the lone pair is placed 1 Å away from the oxygen in the POAV direction. The instantaneous center of mass of the carbons is shown in black, and the instantaneous centers of mass of the hydrogens on the two opposite sides of the graphene sheet are shown in brown. During the simulation run, the closest periodic images of the two ions remained separated by more than 9 Å and their dynamics did not show any correlation with their distance.

interface simple monovalent ions, like Cl^-, do not contribute to the charging nor why the isoelectric point, i.e., the pH value that marks the transition from negative to positive charging, appears to be largely independent of the nature of the surface when the latter does not contain dissociating functional groups.[7] A more satisfactory explanation has been suggested in simulations at the empirical valence bond level[16] or in simulations including an explicit treatment of the electrons at the ab initio density functional level.[12,17] These studies observed that the H^+ complex near a water−vapor interface is oriented so as to expose the lone pair to vacuum, suggesting amphiphilic behavior. A crucial question remains, what is the specific quantitative criterion that could demonstrate why an ion that originates from the hydrophilic H_2O molecule and, in addition, carries a net charge which should make it even more hydrophilic behave like an amphiphilic surfactant?

To address this issue, we report ab initio molecular dynamics simulations of water ion complexes near a hydrocarbon surface.

Results and Discussion

The bulk solvation structures of the water ions have been elucidated by previous ab initio molecular dynamics simulations,[18] which found that the hydronium complex constantly fluctuates between the so-called Eigen H_3O^+ [19] and Zundel $H_5O_2^+$ [20] forms, due to fast proton exchange processes. In the following, we will refer to a nonspecific form of hydronium as H^+. The OH^- ion binds instead to four neighboring molecules forming a more stable complex that resembles a square pyramid with the oxygen of OH^- at its apex,[18] a structure supported by neutron diffraction data.[21,22] Ab initio simulations also showed that the hydrogen of OH^- has a much weaker bond donation affinity than regular H_2O molecules.[18,23] OH^- diffusion occurs when a proton of a solvating H_2O is transferred to OH^-. This process is less frequent than the proton transfer driving the Eigen/Zundel interconversion of hydronium. Thus, H^+ has a higher mobility than OH^-, while both ions have higher mobility than the water molecules.[23] Notably, the solvation structures of the water ions were found to be essentially independent of the quantum vs classical treatment of the nuclei.[18]

In ab initio molecular dynamics[24] the potential energy surface is constructed on the fly from the quantum mechanical instantaneous ground state of the electrons within Kohn−Sham density functional theory.[25] This approach describes accurately the diffuse character of the electronic charge and the polarization effects, which play a crucial role in the formation of the hydrogen bonds (H-bonds). In addition, chemical bonds are

(16) Petersen, M. K.; Iyengar, S. S.; Day, T. J. F.; Voth, G. A. *J. Phys. Chem. B* **2004**, *108*, 14804.
(17) Iyengar, S. S.; Day, T. J. F.; Voth, G. A. *Int. J. Mass. Spectrom.* **2005**, *241*, 197.
(18) Tuckerman, M. E.; Marx, D.; Parrinello, M. *Nature* **2002**, *417*, 925.
(19) Eigen, M. *Angew. Chem., Int. Ed. Engl.* **1964**, *3*, 1.
(20) Zundel, G. In *The Hydrogen Bond-Recent Developments in Theory and Experiments. II. Structure and Spectroscopy*; Schuster, P., Zundel, G., Sandorfy, C., Eds.; North-Holland: Amsterdam, 1976; pp 683−766.
(21) Botti, A.; Bruni, F.; Imberti, S.; Ricci, M. A.; Soper, A. K. *J. Chem. Phys.* **2003**, *119*, 5001.
(22) Imberti, S.; Botti, A.; Bruni, F.; Cappa, G.; Ricci, M. A.; Soper, A. K. *J. Chem. Phys.* **2005**, *122*, 194509.
(23) Tuckerman, M. E.; Chandra, A.; Marx, D. *Acc. Chem. Res.* **2006**, *39*, 151.
(24) Car, R.; Parrinello, M. *Phys. Rev. Lett.* **1985**, *55*, 2471.
(25) Kohn, W.; Sham, L. J. *Phys. Rev.* **1965**, *140*, A1133.

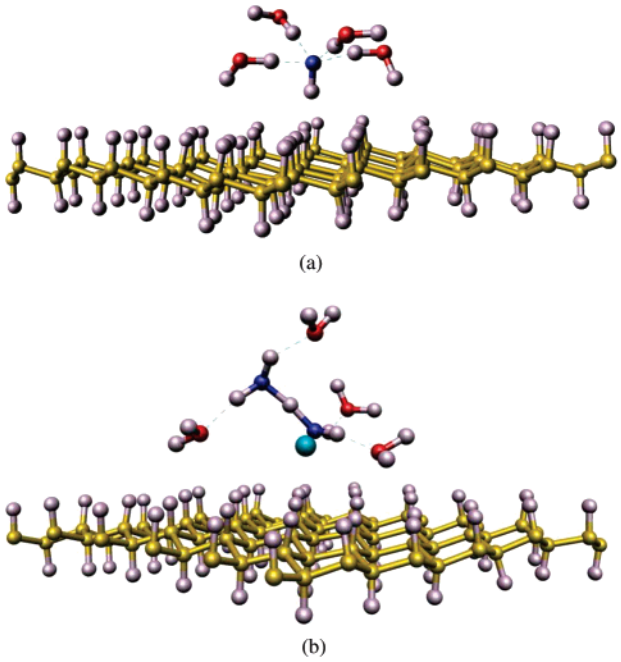

Figure 2. (a) Solvation structure of the hydroxide ion near the hydrophobic surface, showing a side view with the four solvating waters connected by broken lines to the oxygen of the hydroxide. (b). Solvation structure of the hydroniumion near the hydrophobic surface, showing a side view of a Zundel complex with surface and subsurface waters. The four solvating waters are connected to the outer hydrogens of the complex by broken lines. The lone electron pair is shown in cyan.

allowed to break and re-form, an essential feature to model proton exchanges between adjacent molecules. In this study we considered a slab containing 127 waters and 2 ions, OH^- and H^+. The ~18 Å thick water slab was sandwiched between two fully hydrogenated graphene layers representing hydrophobic hydrocarbon surfaces (Figure 1a). All the nuclei were treated classically, and for computational efficiency, the deuterium mass was used for all the hydrogens. We created a hydroxide−hydronium pair by transferring a proton from a molecule on one side of the slab to a molecule on the opposite side of the slab. After electronic relaxation the system was allowed to evolve with rigid water constraints for ~3 ps to stabilize the solvation structures of the ions. Then, the constraints were removed and a ~9 ps long canonical trajectory at $T = 325$ K was recorded. A second trajectory was generated with a similar procedure. In this case we first neutralized the ions at the end of the first trajectory by transferring a proton from H_3O^+ to OH^-. Then we recreated the ions at the two interfaces in the layers of water molecules right next to the hydrogenated graphene, followed by a rigid water run for ~3 ps. Finally, a constraint-free canonical production run at the same temperature was recorded for ~6 ps. In both trajectories the system maintained good diffusive behavior (see Methods for additional details). We should mention that the formal concentration of the ions in our study is 0.4 M. This value is within the range of concentrations utilized in ref 12, which used an ionic concentration of 0.8 M for AIMD runs and an ionic concentration of 0.12 M for classical MD runs. Experimentally, surface spectroscopy was able to detect changes in the vibrational spectra due to water ions only at high concentrations and pH below 2 and above 13.[8] By contrast, ζ potential measurements were significantly more sensitive, showing observable effects in a much wider range of ionic concentrations (10^{-6}−10^{-2} M).[7]

Table 1. Electric Field Projections at Probe Sites

[probe point]	system	field at [...]	std dev
M−P···[$\bar{H}$]	H_2O	0.234	0.024
	H_3O^+ (Eigen)	0.016	0.027
	$H_5O_2^+$ (Zundel)	0.070	0.041
	OH-	0.474	0.093
M−H···[$\bar{P}$]	H_2O	−0.179	0.035
	H_3O^+	−0.344	0.092
	OH^-	−0.021	0.015
	hydrogenated graphene	−0.047	0.019

[a] The field is in e/Å^2 Units. The $\bar{H}$ site is placed 1.8 Å away from O in the O lone pair (P) direction, and the $\bar{P}$ site is placed 2.4 Å away from O in the O−H direction. These distances are based on the neutron diffraction peaks, at 1.8 Å for OH and at 2.8 Å for OO, in water. For the distance between oxygen and the nonbonded Wannier function center, we use the average simulation value of 0.4 Å. We find H^+ to be in the $H_5O_2^+$ configuration approximately 50% of the time. The $\bar{P}$ site of the fully hydrogenated graphene sheet is located along a C−H axis at the same distance from C as the average O−$\bar{P}$ distance in water (2.8 Å). The field due to graphene is calculated by including all the ionic and Wannier charges of the sheet.

Figure 1b shows the evolution of the vertical position of the hydroxide and of the hydronium oxygen, O_{OH^-} and O_{H^+}, respectively. When the hydronium is in the Zundel $H_5O_2^+$ configuration, two oxygens bind covalently to three hydrogens, one of which is shared by the two oxygens. In this case we assign O_{H^+} to the oxygen closest to the shared hydrogen. In agreement with earlier studies[23] proton jumps are more frequent for H^+ than for OH^-. On average we observed an H^+ jump every 0.05 ps and an OH^- jump every 0.1 ps. Remarkably, both the hydrogen of OH^- (green line in Figure 1b) and the nonbonded lone pair of O_{H^+} (red line in the same figure) always point toward the hydrophobic surface when the respective ions reside in the surface layer. This strict correlation is highly local as it disappears when the ions quit the layer of water molecules adjacent to the hydrophobic sheet.

A representative configuration of the interfacial OH^- is shown in Figure 2a. The solvated complex resembles a distorted tetragonal pyramid with the hydrogen of OH^- facing the hydrophobic surface. During the two trajectories in Figure 1b OH^- stayed for 10 ps in the interfacial layer and spent the remaining time in the closest subsurface layer. At the interface proton jumps from neighboring surface molecules are approximately twice as frequent as proton jumps from subsurface water. Surface jumps preserve the orientation and do not lead to H-bond formation between the H of OH^- and the O of an adjacent molecule, which is the most common process in the bulk.[18] Note that we did observe proton jumps to the interfacial OH^- similar to the ones in the bulk, with all these jumps causing the hydroxide to move away from the surface. Such jumps initiated from large fluctuations in the orientation of OH^-. The change in the orientation allowed the H of OH^- to form a hydrogen bond with one of the surface water molecules, which then was followed by a jump of a proton from a subsurface water to OH^-. In spite of the frequent proton jumps, surface OH^- undergoes negligible diffusion because the jumps are almost always followed by return jumps. We could observe only five jumps, always from surface to subsurface, that were not rapidly followed by return jumps. In three cases the ion eventually returned to the surface after staying in the subsurface layer for a time of the order of 1 ps. Subsurface OH^- undergoes substantial diffusion as indicated by a square displacement of 10 Å^2 in 5 ps. Interestingly, this value compares well with a

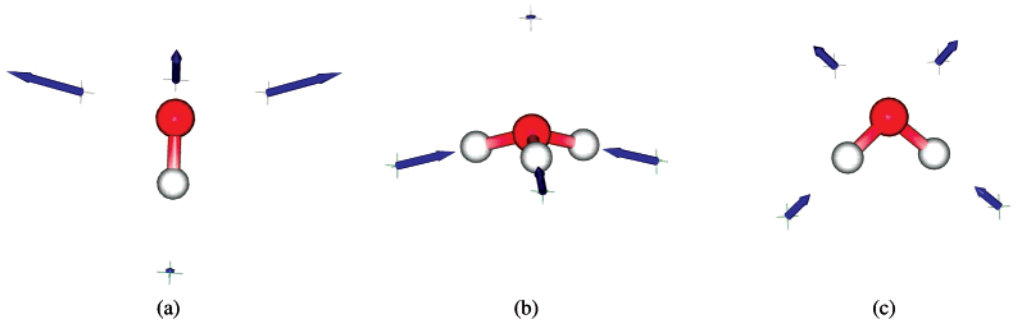

Figure 3. Electric field projections at probe points $\bar{P}$ and $\bar{H}$ for (a) hydroxide, (b) hydronium in the Eigen form, and (c) water. Oxygen is shown in red, and hydrogen in light gray. The distances to the probe points, as well as the lengths of the arrows, are set according to Table 1. Note that as shown, the field vectors are fully 3-dimensional, and therefore, their 2-dimensional lengths seen in the figure depend on how they are oriented with respect to the chosen point of view.

mean square displacement of 1.5 Å^2/ps found in bulk AIMD simulations at 300 K.[23]

In Figure 2b we report a representative configuration of the hydronium at the interface. It is a Zundel form involving surface and subsurface water, and the lone pair of O_{H^+} is facing the hydrophobic surface. In our simulation a fluctuating Zundel/Eigen complex near a planar hydrophobic interface typically involved surface and subsurface water. Frequent surface−subsurface jumps of the O_{H^+} center are evident in both trajectories in Figure 1b. Overall H^+ remained at the interfacial layer for 7 ps, during which little diffusion occurred as indicated by a square displacement of 3 Å^2 in the second trajectory in Figure 1b. Interestingly and in close analogy with the hydroxide case, when H^+ escaped from the interface layer, which happened only once in the first trajectory, it underwent substantial diffusion. The corresponding square displacement was of 14 Å^2 in 8 ps. This value should be compared with a mean square displacement of 2.2 Å^2/ps found in bulk AIMD simulations at 300 K.[23] Also, due to significantly more frequent proton exchange processes with the nearby waters at any given moment, the H^+ complex perturbs a larger number of H-bonds than the OH^-. This observation appears to be consistent with the spectroscopic data for the water−air interface,[8] where at similar ionic concentrations larger effects are observed for hydronium compared to hydroxide ions.

To understand why the water ions orient themselves near a hydrophobic surface we developed a criterion to quantify the directional H-bond affinity of a chemical species M. An H-bond between M and an adjacent molecule M* involves either a lone pair (P) of M and an H of M* (M−P···H) or an H of M and a lone pair of M* (M−H···P). We indicate the sites that *can be* occupied by a lone pair P or an H of M* by $\bar{P}$ and by $\bar{H}$, respectively. Then, given the predominantly electrostatic origin of the hydrogen bonds, a good indicator of the H-bond affinity of a $\bar{P}$ or an $\bar{H}$ site is given by the projection of the electric field generated by M at this site on the corresponding H-bond direction, defined by the M−H or the M−P vector.

To compute the electric field due to an individual molecule in the liquid, we need to partition the delocalized quantum charges of the condensed phase into individual molecular contributions. In order to do so, we apply to a representative subset of molecular configurations the unitary transformation that converts valence electronic orbitals into maximally localized Wannier functions (MLWF).[26] While the valence orbitals are typically delocalized over the entire simulation box, four distinct MLWFs are uniquely associated with each individual water molecule. Two of these four MLWFs represent bond pairs and have their centers on the O−H bonds; the other two represent lone pairs, and their centers define the O-lone pair axes.[27] Using the four MLWF centers (−2e each) and the charges of the ionic cores (+6e for O and +1e for each H), a dipole can be associated to each liquid molecule. These dipoles and their correlations allow us to compute physical observables, such as infrared intensities[28] and the dielectric permittivity of liquid and solid water.[29] In this case we use the MLWF centers and ion charges of each molecule to compute the electric field at the $\bar{P}$ and $\bar{H}$ sites. The field calculated in this way is a good approximation of the true field of the molecule at these sites. The same procedure is readily applied to H^+, OH^-, and the fully hydrogenated graphene sheet.

The median simulation values of the field projections at the various probe sites are reported in Table 1, in which we list separately the results for water, for OH^-, for the Eigen H_3O^+ and Zundel $H_5O_2^+$ forms of H^+, and for hydrogenated graphene. Several considerations are in order. The field due to the fully hydrogenated graphene sheet is an order of magnitude smaller than that of a water molecule, illustrating the hydrophobic nature of the sheet. The results for the ions are most illuminating. While the $\bar{P}$ site of OH^- and the $\bar{H}$ site of H^+ are close in hydrophobicity to the $\bar{P}$ site of graphene, the $\bar{H}$ sites of OH^- and the $\bar{P}$ sites of H^+ are strongly hydrophilic, even more so than the corresponding sites of the H_2O molecules, eloquently revealing the amphiphilic character of the ions (see Figure 3 for a graphic representation of this finding). What happens can be simply stated as follows. When a polar water molecule looses/gains a proton (+1e) to become a water ion, the acquired charge is located off center with respect to O and contributes a field that nearly cancels the field of the original polar molecule at one of its H-bonding sites while significantly reinforcing it at all other sites. Thus, the surfactant-like behavior of the ions is a direct consequence of the asymmetry of their charge distribution.

The previous analysis, though qualitative, is robust. It should not depend on such details as the adopted DFT approximation, since adopting a different exchange-correlation functional should not alter the charge distribution in any major way. Nor should

(26) Marzari, N.; Vanderbilt, D. *Phys. Rev. B* **1997**, *56*, 12847.
(27) Silvestrelli, P. L.; Parrinello, M. *Phys. Rev. Lett.* **1999**, *82*, 3308.
(28) Sharma, M.; Resta, R.; Car, R. *Phys. Rev. Lett.* **2005**, *95*, 187401.
(29) Sharma, M.; Resta, R.; Car, R. *Phys. Rev. Lett.* **2007**, *98*, 247401.

it depend on the time span of the simulation, which is sufficient to sample accurately the local equilibrium charge distribution. On the other hand, properties like the relative abundance of Zundel and Eigen configurations and/or the surface pH are more likely to depend sensitively on the adopted approximations. Our simulation (see Figure 1B) shows that when the water ions are located at the interface of water with hydrogenated graphene, they have a reduced tendency to move away from it, in spite of the frequent proton-transfer processes. Interfacial localization severely hampers ion diffusion, which becomes substantial only when the ions move away from the surface layer. Given the accessible time span of the simulation, these observations merely suggest a positive surface affinity of the ions, a quantitative estimate of which could only be obtained from potential of mean force calculations like those of ref 30.

Conclusions

In summary, we have carried out ab initio molecular dynamics simulations of water ion complexes near a water−hydrophobic interface. We find that not only hydroniums but also hydroxides behave like amphiphilic surfactants.[31] We understand the origin of this behavior using a novel criterion to measure the hydrogen bond affinity of a molecular system. We find that the molecular charge distribution gives rise to hydrophobic and hydrophilic sides in both water ions, a fact that is revealed by directly probing the electric field at the respective hydrogen bond donor/acceptor sites. In addition, H^+ tends to delocalize between surface and subsurface layers as a consequence of the Grotthus shuttle mechanism,[32] while OH^- is more localized in the surface layer. These observations suggest possible causes for the higher surface affinity of the hydroxide compared to the hydronium, which was found in the ζ potential measurements.[7] We stress that in this work we have only investigated the water−hydrogenated graphene interface. Further studies are required to find out if similar effects also occur at other interfaces between water and a medium that is hydrophobic in nature, such as, e.g., the water−air interface.

In addition to affecting hydrophobic interactions,[33,34] the amphiphilic character of the water ions and the charging of water−hydrophobic interfaces could play a key role in the tribocharging processes observed upon metal−hydrophobic polymer contact.[35] More than a century ago it was suggested that the charge separation occurring when two surfaces are brought into contact originates from the surface preference for H^+ and OH^- ions that reside in the adsorbed water at the surfaces.[36,37] Our work supports this hypothesis by suggesting a microscopic mechanism for the presence of negative surface charge in hydrophobic polymers. This effect is further confirmed by the correlation between the magnitude of the observed static charge transfer and the surface ζ potential of a polymer.[38]

Methods

The three-dimensional periodic simulation cell is hexagonal in the graphene plane (side 15.265 Å). The vertical dimension is 24.0 Å, based on constant pressure simulations under zero applied external pressure for a similar slab made of pure water. Under these conditions the average density at the center of the slab is close to the bulk experimental density. In the electronic structure calculation we used the BLYP GGA functional,[39,40] ultrasoft pseudopotentials[41] for all the atoms (H, C, and O), and a plane wave representation of the wave functions with a kinetic energy cutoff of 25 Ry. The cutoff for the smooth electronic density was 100 Ry, and the augmented density cutoff was 200 Ry. All the atoms were allowed to move. The trajectories were generated with the CP code of the ν-Espresso package. In the integration of the Car−Parrinello equations of motion,[24] we adopted a fictitious electron mass of 700 au and a time step of 10 au.[42] Canonical simulations were carried out with "massive" Nose Hoover chains[43] (4 thermostats in each chain, with frequencies of 12, 9, 6, and 3 THz), setting the temperature to 325 K. With this choice of parameters the fictitious kinetic energy of the electrons did not show any appreciable drift and the water remained diffusive throughout the simulation (the calculated diffusion coefficient was $D = \sim 1.3 \times 10^{-9}$ m^2/s, to be compared with an experimental value of $\sim 1.86 \times 10^{-9}$ m^2/s for heavy water at room temperature[44]).

Acknowledgment. This material is based upon work supported in part by the U.S. Army Research Office Multidisciplinary University Research Initiative (ARO/MURI) under Grant No. W911NF-04-1-0170. A computer time grant from the TIGRESS High Performance Computing Center at Princeton University is also acknowledged.

JA077205T

(30) Li, J. L.; Car, R.; Tang, C.; Wingreen, N. S. *Proc. Natl. Acad. Sci.* **2007**, *104*, 2626.
(31) Wennerstrom, H.; Lindman, B. *Phys. Rep.* **1979**, *52*, 1.
(32) de Grotthuss, C. J. *T. Ann. Chim.* **1806**, *LVIII*, 54.
(33) Meyer, E. E.; Lin, Q.; Hassenkam, T.; Oroudjev, E.; Israelachvili, J. N. *Proc. Natl. Acad. Sci.* **2005**, *102*, 6839.
(34) Meyer, E. E.; Rosenberg, K. J.; Israelachvili, J. *Proc. Natl. Acad. Sci.* **2006**, *103*, 15739.
(35) Wiles, J. A.; Grzybowski, B. A.; Winkleman, A.; Whitesides, G. M. *Anal. Chem.* **2003**, *75*, 4859.
(36) Knoblauch O. *Z. Phys. Chem.* **1902**, *39*, 225.
(37) Harper, W. R. *Contact and Frictional Electrification*; Clarendon Press: Oxford, U.K., 1967.
(38) McCarty L. S.; Whitesides G. M. *Angew. Chem., Int. Ed. Engl.* **2008**, Early View.
(39) Becke, A. D. *Phys. Rev. A* **1988**, *38*, 3098.
(40) Lee, C. T.; Yang, W. T.; Parr, R. G. *Phys. Rev. B* **1988**, *37*, 785.
(41) Laasonen, K.; Car, R.; Lee, C.; Vanderbilt, D. *Phys. Rev. B* **1991**, *43*, 6796.
(42) Sit, P. H. L.; Marzari, N. *J. Chem. Phys.* **2005**, *122*, 204510.
(43) Tobias, D. J.; Martyna, G. J.; Klein, M. L. *J. Phys. Chem.* **1993**, *97*, 12959.
(44) Hardy, E.; H.; Zygar, A.; Zeidler, M. D.; Holz, M.; Sacher, F. D. *J. Chem. Phys.* **2001**, *114*, 3174.
(45) Haddon, R. C.; Scott, L. T. *Pure Appl. Chem.* **1986**, *58*, 137.